Reply to the comments of anonymous **reviewer #1** on the manuscript *essd-2017-36*
"A multi-decadal wind-wave hindcast for the North Sea 1949–2014: coastDat2" by Nikolaus Groll and Ralf Weisse

We thank the anonymous reviewer #1 for her/his comments, which helped to improve the manuscript.

In the following, the referee's comments are shown in blue.

This manuscript presents a new multi-decadal wind-wave hindcast for the North Sea. The hindcast spans 1949-2014 and forms part of the CoastDat database. The hindcast provides a long record (60 years) at relatively high spatial resolution (3 nautical miles). The study assesses the skill of the hindcast relative to a set of in-situ platform and buoy wave observations in the North Sea. The earliest data to which a validation was carried out were two observation points (EKO and K13) both commencing in 1980. The performance of the hindcast was compared to the skill of wave fields derived from the ECMWF ERA-Interim reanalysis. Key differences between the datasets are displayed in Figure 6, where the CoastDat2 hindcast displays a tendency to overestimate observed wave heights, whereas ERA-Interim fields slightly underestimate significant wave heights. This is presented as a potential benefit for the database in providing a conservative estimate for extreme wave heights in the North Sea for planning purposes. In general however, Table 2 suggests ERA-Interim has greater skill relative to observations than the presented CoastDat2 database.
Despite the ERA-Interim database demonstrating greater skill in the region of interest, the paper argues the extended time-series, the high spatial resolution, and the overestimated (conservative) extreme wave height estimates provide a distinctive dataset which will be of value to the user community in the North Sea. While the high spatial resolution offers value, I have reservations about the merit of the extended time-series given no investigation of the skill of the hindcast to represent trends (against long independent datasets) or of the homogeneity of the dataset has been carried out on the database. Given this shortcoming, my recommendation is the study undergo major revision before being published. This revision should include some consideration of the skill of the full temporal extent of the time-series.

The main concern of the reviewer is "reservations about the merit of the extended time-series given no investigation of the skill of the hindcast to represent trends (against long independent datasets) or of the homogeneity of the dataset has been carried out on the database". The argument is reasonable although, because of the lack of long-term wave measurements, it can be addressed only indirectly: The wave climate strongly depends on the wind climate and the quality and homogeneity of the wave hindcast is thus strongly coupled to those of the driving atmospheric data which are discussed in Geyer (2014) and in Geyer et al. (2015). In these papers, hindcast wind is compared with observations and for most locations, a slight overestimation and root mean square errors between 1.6 ms^{-1} and 3.4 ms^{-1} were found. Moreover, the long-term (decadal) variability described closely resembles that known from variations in storm activity over the North Sea. The latter was shown to occur also for waves in a hindcast that uses wind fields from a different regional atmosphere model that was, however, driven by the same global reanalysis (Weisse and Günther (2006).

Regarding homogeneity Kistler et al. (2001) investigated the issue for the global NCEP reanalysis that provided the boundaries for the regional atmosphere models used in this and the study of Weisse and Günther (2006). Kistler et al. (2001) showed that for the Northern Hemisphere rapidly increased from 1948 to 1958 while there is only a small increase afterwards. The latter implies that the driving global reanalysis is mostly homogeneous for our area after about 1958 and as there were no changes in regional model systems used in Geyer (2014) and our study we conclude that the same also holds for our wave hindcast.

To address the reviewers concern we have added a corresponding paragraph in the revised manuscript.

We have not included analysis of long-term variability and trends as the main focus of this manuscript is to introduce this new wave hindcast. For the brevity of the manuscript, we focused on the overall capability of the wave hindcast to represent the wave climate and statistics. Value to users of such long-term data sets is described in Weisse et al. (2009) and Weisse et al. (2015).

Other than this consideration, the paper is generally well written and clear. I have only a few further minor comments which I would also like to see considered in the revised version of the manuscript.
Abstract: Second sentence. No statistics have yet been introduced.

We modified the corresponding sentence in the abstract accordingly.

Some revision of English is required.

We carefully checked the manuscript for possible errors.

Figures 2, 6 and 7. Please label x and y axes, as opposed to including information in caption.

We added axis labels to the figures.

Figures 4, 5 and 8. Please provide some axis information, in order to resolve spatial scales.

We added an axis scale to the figures.

An equivalent table to Table 2, 3 and 4 for directional information would add benefit.

We added a table with the error metrics for the wave direction.

References:

Geyer, B.: High-resolution atmospheric reconstruction for Europe 1948–2012: coastDat2, Earth System Science Data, 6, 147–164, 30, doi:10.5194/essd-6-147-2014, http://www.earth-syst-sci-data.net/6/147/2014/, 2014

Geyer, B., Weisse, R., Bisling, P., and Winterfeldt, J.: Climatology of North Sea wind energy derived from a model hindcast for 1958–2012, Journal of Wind Engineering and Industrial Aerodynamics, 147, 18 – 29, doi:http://dx.doi.org/10.1016/j.jweia.2015.09.005, http://www. sciencedirect.com/science/article/pii/S0167610515002214, 2015.

Kistler, R., Collins, W., Saha, S., White, G., Woollen, J., Kalnay, E., Chelliah, M., Ebisuzaki, W., Kanamitsu, M., Kousky, V., van den Dool, H., Jenne, R., and Fiorino, M.: The NCEP–NCAR 50–Year Reanalysis: Monthly Means CD–ROM and Documentation, Bulletin of the American Meteorological Society, 82, 247–267, doi:10.1175/1520-0477(2001)082<0247:TNNYRM>2.3.CO;2, http://dx.doi.org/10. 1175/1520-0477(2001)082<0247:TNNYRM>2.3.CO;2, 2001.

Weisse, R. and Günther, H.: Wave climate and long-term changes for Southern North Sea obtained from a high-resolution hindcast 1958-2002, Ocean Dynamics, 57, 161–172, doi:10.1007/s10236-006-0094-x, 2007.

Weisse, R., von Storch, H., Callies, U., Chrastansky, A., Feser, F., Grabemann, I., et al.: Regional Meteorological-Marine Reanalyses and Climate Change Projections: Results for Northern Europe and Potential for Coastal and Offshore Applications. In: Bull. Amer. Meteor. Soc. 90 (6), S. 849–860. DOI: 10.1175/2008BAMS2713.1., 2009.

Weisse, R., Bisling, P., Gaslikova, L., Geyer, B., Groll, N., Hortamani, M., Matthias, V., Maneke, M., Meinke, I., Meyer, E. M., Schwichtenberg, F., Stempinski, F., Wiese, F., and Wöckner-Kluwe, K.: Climate services for marine applications in Europe, Earth Perspectives, 2, 25, 1–14, doi:10.1186/s40322-015-0029-0, http://dx.doi.org/10.1186/s40322-015-0029-0, 2015.

A multi-decadal wind-wave hindcast for the North Sea 1949 – 2014: coastDat2

Nikolaus Groll[1] and Ralf Weisse[1]

[1]Institute for Coastal Research, Helmholtz-Zentrum Geesthacht, 21502 Geesthacht, Germany

Correspondence to: Nikolaus Groll (nikolaus.groll@hzg.de)

Abstract.

Long and consistent wave data are important for analysing wave climate variability and change. Moreover, such ~~statistics~~ data are also needed in coastal and offshore design and for addressing safety-related issues at sea. Using the third-generation spectral wave model WAM a multi-decadal wind-wave hindcast for the North Sea covering the period 1949–2014 was produced. The hindcast is part of the coastDat database ~~representing~~ which represents a consistent and homogenous met-ocean ~~data set~~dataset. It is shown that despite not being perfect, data from the wave hindcast are generally suitable for wave climate analysis. In particular comparisons of hindcast data with in situ and satellite observations show on average a reasonable agreement while a tendency towards overestimation of the highest waves could be inferred. Despite these limitations, the wave hindcast still provides useful data for assessing wave climate variability and change as well as for risk analysis, in particular when conservative estimates are needed. Hindcast data are stored at the World Data Center for Climate (WDCC) and can be freely accessed using the doi:10.1594/WDCC/coastDat-2_WAM-North_Sea (Groll and Weisse, 2016) or via the coastDat web-page http://www.coastdat.de.

1 Introduction

Multi-decadal wind-wave hindcasts have become a common tool in supporting the assessment of wave climate variability and change, such as its extremes, trends or seasonal and inter-annual to decadal variability (e.g. WASA-Group, 1998; Sterl et al., 1998; Cox and Swail, 2001; Weisse and Günther, 2007; Dodet et al., 2010). Data from wind-wave ~~hindcast data~~ hindcasts are also frequently used in practically oriented applications such as in navigation, shipbuilding, offshore design or strategic planning of logistics for the operation of future offshore wind farms (Weisse et al., 2009, 2015). Further applications comprise studies such as evaluating the impact of waves on sea salt emissions (Neumann et al., 2016) or the evaluation of the potential success or failure of different response strategies to oil pollution (Schwichtenberg et al., 2016). For all these different types of applications long, homogeneous and consistent wind-wave data are needed to derive robust estimates of wind-wave related parameters specific to the problem. Often such information is unavailable from in situ or satellite data alone and multi-decadal wind-wave hindcasts have become a common approach in complementing such analyses.

While formerly wind-wave hindcasts were developed independently using atmospheric forcing available at that time, they nowadays form an integral part of global atmospheric reanalysis systems (e.g. Dee et al., 2011; Chawla et al., 2013). Owing to the limited spatial and temporal resolution of such global reanalyses, there is, however, still a substantial number of regional efforts aiming at higher spatial and temporal resolution. These efforts usually use the traditional approach in which downscaled global reanalysis wind fields are subsequently used to run a wave hindcast system over the reanalysis period or sub-periods within that period (e.g. Charles et al., 2012; Reguero et al., 2012, 2013; Bertin et al., 2013; Ponce de León and Guedes Soares, 2015).

For the North Sea, there presently exist a number of wind-wave hindcasts covering at least some decades of years. The first of these multi-decadal hindcasts was, to our knowledge, developed within the WASA project (WASA-Group, 1998) while a more recent approach based on the ERA-40 global atmospheric reanalysis (Uppala et al., 2005) is described in Reistad et al. (2011). Aiming at a consistent description of met-ocean conditions in the North Sea Weisse and Günther (2007) developed and described a multi-decadal wind-wave hindcast for the southern North Sea that is part of a comprehensive met-ocean downscaling known as coastDat1 (Weisse et al., 2009). The latter ~~is based on~~ used the global NCEP/NCAR reanalysis (Kalnay et al., 1996) as boundary conditions and provides a consistent met-ocean ~~data set~~ dataset comprising of regionally downscaled atmospheric (Feser et al., 2001), tide-surge (Weisse and Plüss, 2006) and wind-wave ~~Weisse and Günther (2007)~~ (Weisse and Günther, 2007) conditions from which full met-ocean data are available for every hour over the hindcast period.

Data from coastDat1 were extensively used for a wide variety of studies. For an overview see for example Weisse et al. (2009). While there was and there still is substantial interest in these data, the effort terminated in 2007 when the atmospheric component of the met-ocean hindcast was discontinued and consistent atmospheric data to drive the wind-wave and tide-surge models became unavailable. Up to that time, data from coastDat1 have been used by more than 50 different users with a large variety of applications. About 50 % of these users originated from commercial enterprises, while about 25 % had a more direct scientific interest and another 25 % came from public authorities (Weisse et al., 2015). Because of ongoing interest in both, the scientific and the commercial exploitation of the data, eventually a ~~following-up~~ follow-up effort called coastDat2 was initiated. In this effort, upgraded models with higher spatial resolution were used and the wind-wave part, in addition, now also covered the entire North Sea. The atmospheric component of coastDat2 is described in Geyer (2014). In the following, we describe and evaluate the upgraded wind-wave part (Groll and Weisse, 2016) that is driven by the coastDat2 wind fields (Geyer, 2014).

2 Model setup

For the wind-wave hindcast in coastDat2 the third-generation spectral wind-wave model WAM (WAMDI-Group, 1988; Komen et al., 1996) version 4.5.4 was used. This version represents an update and extension of the WAM cycle 4 used in coastDat1 (Weisse and Günther, 2007) the details of which are described in the WAM documentation available at http://mywave.github.io/WAM/. Apart from some technical changes such as in the I/O routines, a major change was introduced by the replacement of the wave dissipation source term with a new version described in Bidlot et al. (2005) and Bidlot et al. (2007).

For the coastDat2 hindcast, the wave model was used in a nested version with a coarse grid simulation covering most of the northeast North Atlantic and a fine grid simulation covering the North Sea from 4.75°W –13.25°E and from 50.5°N –59.5°N

(Figure 1). The grid size of the coarse grid is 0.5°latitude x 0.75°longitude while that of the fine grid nested within the coarse grid is 0.05°latitude x 0.075°longitude. The latter corresponds to a grid spacing of approximately 3-by-3 nautical miles.

Wave spectra were computed and discretised using 35 frequencies ranging from approx. 0.042 Hz to 1.067 Hz and 24 directional bins. The integration time step was set to three minutes and integrated parameters derived from the wave spectra such as significant wave height, mean period or direction were calculated and stored at every full model hour while wave spectra were only kept every three hours. Boundary conditions were transferred from the coarse to the fine grid every hour using the full modelled wave spectra. For both grids, the model was set-up and integrated in shallow water mode including depth refraction and depth-induced wave breaking. In the coarse grid simulation also monthly sea ice conditions from the northeast North Atlantic were included to account for the varying fetch arising from variations in sea ice coverage.

3 External data

3.1 Forcing data

For both, the coarse and the fine grid wind-wave simulations near-surface marine wind fields at 10m height were used. These wind fields take effects from varying atmospheric stability into account and were obtained from the high-resolution regional atmospheric hindcast described in (Geyer, 2014) Geyer (2014) as part of coastDat2. For the production of this atmospheric hindcast, the regional atmosphere model COSMO-CLM (Rockel et al. 2005) with a spectral nudging scheme (von Storch et al., 2000) was used to dynamically downscale the global atmospheric conditions given by the driving NCEP/NCAR reanalysis (Kalnay et al., 1996; Kistler et al., 2001). The downscaling was performed for the North Atlantic/ European region and the model was integrated on a rotated grid with a grid size of 0.22° x x 0.22°corresponding to a spatial resolution of about 25-by-25 km. Atmospheric wind fields to drive the wave model were available and used every model hour. Validation of the atmospheric hindcast is described in Geyer (2014). Compared to the driving global reanalysis an improved representation of marine wind speeds in coastal areas, especially for higher wind speeds, is noted (Geyer et al., 2015). Note that the atmospheric hindcast described in Geyer (2014) ends in 2012 but was extended for the present study to provide consistent data until the end of 2014.

For the coarse grid simulation , in addition, monthly sea ice concentrations provided by the Hadley Centre Sea Ice and Sea Surface Temperature data set dataset (HadISST1.1, Rayner et al., 2003) were used. The sea ice concentrations had a spatial resolution of 1° x x 1°and were spatially interpolated to the coarse wave model grid. Subsequently in the simulation sea ice was accounted for by treating all model grid points with sea ice concentrations exceeding 50 % as land for the corresponding time steps.

3.2 Reference data

A number of in situ wind-wave observations from platforms and buoys in the North Sea originating from different sources were available for validation (Table 1). Basic quality control was applied but no attempt to check homogeneity was done. The data cover different time periods including gaps and differ in their temporal resolution. Because the model output is available only at full model hours, the comparison with observations was limited to data that were measured within ± 10 minutes around full hours.

In addition, wind-wave data derived from satellite provided by the merged altimeter wave height database version 11.0 (Queffeulou, 2013) were used. These data originate from the GlobWave project (http://www.globwave.org) and cover the period 1991 to present. The satellite data were co-located with the model data using a co-location criteria of ± 10 minutes at which the position of the satellite was matched with the nearest grid point of the wave model.

To compare the wave model results in space and time ~~also~~ data from the ERA-Interim global reanalysis (Dee et al., 2011) spatially interpolated to the coastDat2 wave model grid were used. More specifically, data from the ocean wave product of ERA-Interim were used, which employs the same wave model as used in this study. ERA-Interim wave data are available every six hours at 00, 06, 12 and 18 UTC and at a spatial resolution of 0.75° latitude × 0.75° longitude. ~~Data are available from 1980 onwards. From~~ Wind data from satellites and in situ observations are assimilated into ERA-Interim. Further, from 1990 onwards wave spectra ~~in ERA-Interim~~ were adjusted using altimeter data~~(Dee et al., 2011).~~. Wave buoy data were not used in the assimilation procedure (Dee et al., 2011). For comparison, we use the ERA-Interim wave data from 1980 to 2014.

In order to avoid biases, only those instances in time are used for comparison for which both, observations and hindcast data were simultaneously available. In particular, this results in comparison of hourly/six-hourly data when coastDat2 hindcast/ERA-Interim reanalysis is involved.

4 Evaluation

For the evaluation of the wave hindcast the following error metrics were applied: the mean, the standard deviation (SD), the bias, the root mean square error (RMSE), the scatter index (SI) ~~,~~ and the correlation coefficient (r). To evaluate the unbiased RMSE the standard deviation of the error (SDE) was used. All measures were calculated for the entire datasets if not stated otherwise. In the following, measures are called errors when simulations are compared with observations and are called differences when the two simulations are compared. Further details of the error metrics can be found in Appendix A.

4.1 Significant wave height

Significant wave height (SWH) derived from hindcast data and in situ measurements was compared at seven sites in the North Sea (Figure 2). Comparison of instantaneous values revealed noticeable scatter between modelled and observed data with biases ranging between about 0 and 0.25 m. Root mean square errors varied between approximately 0.4 and 0.7 m (Table 2). When distributions were compared, generally a reasonable agreement was inferred for the lower to intermediate percentiles corresponding to wave heights of up to 2 – 4 m depending on location (Figure 2). Higher percentiles were generally found to be overestimated in the hindcast data.

To put these findings into perspective Figure 2, in addition, shows a corresponding analysis for SWH derived from the ERA-Interim reanalysis. Here generally a tendency towards an underestimation of the higher SWHs can be inferred. This feature is most pronounced at near coastal locations such as at station ELB. An evaluation with a normalised Taylor-diagram (Figure 3) indicates that for both, the ERA-Interim and the coastDat2 SWHs correlation with observations typically vary around about 0.9 with the values being slightly higher for the ERA-Interim reanalysis. The analysis further reveals that the observed SWH variability is somewhat underestimated by the ERA-Interim reanalysis and overestimated in the coastDat2 ~~data set~~dataset. The centred root mean square errors are slightly above (below) 0.5 m for coastDat2 (ERA-Interim). ~~No substantial differences in conclusions are obtained when~~ Comparing 6-hourly instead of hourly values for the coastDat2 SWHs ~~are used~~reveals no substantial differences in Taylor diagram statistics. A more detailed comparison of error statistics for the seven locations is provided in Table 2.

A spatial comparison of the differences between ERA-Interim and coastDat2 SWHs for the common period 1980 – 2014 is illustrated in Figure 4. With the exception of near-coastal waters, the SWH obtained from the coastDat2 hindcast is on average higher compared to that from the ERA-Interim reanalysis with increasing differences from south to north. Largest systematic differences of up to 0.6 m were found off the Norwegian coast. A similar spatial pattern is obtained when root mean square differences are compared. These differences were found to vary between about 0.4 m in the southern North Sea and more than 0.9 m in the northern parts of the model domain. When the bias is removed from the root mean square differences, again a similar pattern for the standard deviation of differences with somewhat smaller values compared to the root mean square differences is obtained.

When the spatial comparison is made with the SWHs derived from the GlobWave satellite dataset instead of ERA-Interim, differences are less distinct but still present (Figure 5). Similar spatial features but with smaller values are found in the southern North Sea and near the coasts. The latter corresponds to too small wave heights in ERA-Interim when compared to GlobWave data (not shown). Although the underestimation may reach values of up to 0.4 m on average, the magnitude of the systematic differences between ERA-Interim and GlobWave is still smaller than that between the coastDat2 and the GlobWave data. Note that the robustness of these results is limited, as the number of available satellite data is small. For most of the domain less than 100 co-located data points were available for the comparison. This corresponds to only about one-tenth of a percent of the potentially available hourly values within the period 1992 – 2014.

To obtain a more robust figure an additional comparison of co-located data from GlobWave and coastDat2 was made taking all co-located data irrespective of their location into account. The results are shown in Figure 6 and corresponding error statistics are presented in Table 2. Altogether, errors statistics obtained and conclusions derived from this exercise are similar to those based on comparison with in situ observations. Values for bias and RMSE are slightly enhanced compared to those derived from comparison with in situ observations. This can be attributed to the fact that most of the in situ observations were taken in the southern part of the North Sea where error statistics of the coastDat2 hindcast are smaller, while the more northern parts with larger errors have a stronger weight in the GlobWave comparison.

4.2 Wave period

Different definitions for wave periods are used depending on the specific analysis. Here two of the more frequently used measures are used for comparison with observations: (i) the mean zero crossing period derived from the zeroth and second-order moment of the spectrum (T_{m02}) and (ii) the mean wave period (MWP) defined by the ratio of the first and zeroth-order moment of the spectrum corresponding to the total energy of the wave spectrum (Holthuijsen, 2007). The Comparison is made based on the availability of the different ~~data sets~~datasets.

When observed and hindcast T_{m02} periods are compared, an underestimation (overestimation) for short (long) periods can be inferred for most locations (Figure 7). Deviations are mostly small and typically in the order of 0.5 s, except for the near shore location WES. Despite the scatter for instantaneous values, hindcast wave periods on average show a good agreement with the observations. The larger deviations occurring at the location WES are probably related to the relatively shallow water depth which might lead to too small wave dissipation caused by missing small scale bathymetric features not resolved at the given spatial resolution of the wave hindcast model.

A spatial comparison of the MWPs from the coastDat2 hindcast and the ERA-Interim reanalysis for the period 1980–2014 is presented in Figure 8. On average the coastDat2 hindcast shows longer MWP (up to more than 0.6 s) for large areas of the North Sea with the largest differences occurring in the deeper waters in the northeastern part of the model domain. In coastal areas, differences are mostly less pronounced. For the root mean square differences and the standard deviation of the differences similar spatial patterns can be inferred.

A comparison between T_{m02} period measures derived from observations and the coastDat2 hindcast is presented in Table 3. The MWP measures between observations, coastDat2 hindcast and the ERA-Interim reanalysis is presented in Table 4. It can be inferred, that compared to observations T_{m02} periods are on average underestimated in the coastDat2 hindcast while MWPs are on average overestimated. For ERA-Interim no T_{m02} data were available. MWPs are similarly biased high although with somewhat smaller values. Variability is generally overestimated in both model simulations with the ERA-Interim errors again being smaller.

4.3 Wave direction

A comparison between mean wave directions derived from coastDat2, ERA-Interim and observations was performed at three locations (Figure 9). Generally, a good agreement was inferred. At FN1 a more systematic deviation for mean wave directions coming from southerly directions was obtained. Both model data, coastDat2 and ERA-Interim, show the same systematic error. This may point to some bathymetric effects that remain unresolved at the chosen model resolution or to the installation of wave measurements that might be sheltered from certain wave directions.

4.4 Individual extreme events

In order to illustrate the amount of agreement and disagreement described above in a more direct and accessible way, modelled and observed wave parameters during an extreme wave event were compared. Here we used the event generated by the extra-tropical storm Britta (31 October 2006 – 1 November 2006) which caused some structural damage at the platform FINO1 (Kettle, 2015). Visual inspection of time series of significant wave height, wave periods and direction reveals that while the overall development for the days around the storm is reasonably captured by both, the coastDat2 hindcast and the ERA-Interim reanalysis, both data sets datasets substantially underestimate the peak significant wave height that occurred during the storm (Figure 10).

The underestimation is less severe in the coastDat2 hindcast and substantially more pronounced in the ERA-Interim reanalysis. Inspection of the time series further shows, that during less stormy periods ERA-Interim data are generally closer to the observations while positive systematic errors are obvious for the coastDat2 hindcast. In detail and for the time series shown it was found that (i) peak significant wave heights appear to be better represented in the coastDat2 hindcast while there generally appears to be a too rapid increase towards the extremes, (ii) during times with small wave periods the T_{m02} period appears to be reasonable in the coastDat2 simulation while again a too rapid increase towards the extremes is observed, (iii) for the MWP a systematic bias towards too high values is clearly visible that is substantially less pronounced in the ERA-Interim data and (iv) mean wave directions are very well represented in both simulations.

Extreme value analyses are often based on maximum values occurring within an interval for which a given threshold is exceeded. For the analysis, the exact timing of the extreme within this interval is less important. In order to assess the representativeness of such extremes in the modelled data setdataset, we defined the duration of an extreme event as the time period for which the SWH exceeded the 95th percentile of the observed SWH and sampled the maximum SWHs that occurred during that interval from all data setsdatasets; that is, the observations, coastDat2 and ERA-Interim. The analysis was performed exemplary for station FN1. It was found that coastDat2 overestimated the observed maximum SWH by 0.38 m with an RMSE of 1.12 m. ERA-Interim on the other hand underestimated the observed maximum SWH by -0.63 m but showed a smaller RMSE of 0.81 m. While the underestimation of ERA-Interim extremes could partly be related to the coarser temporal resolution of six hours, the result indicates that for extreme value analyses data from coastDat2 would provide a more conservative estimate.

5 Conclusions

To our knowledge, the described data set dataset represents the longest regional reconstruction of wind-wave climate for the North Sea based on dynamically downscaled high-resolution atmospheric reanalysis data. It covers more than 60 yearsand ,, provides hourly integrated wind-wave parameters and spectral wave information every three hours at a spatial resolution of approximately 3-by-3 nautical miles and delivers a comprehensive set of wave parameters (Appendix B).

Altogether the reconstructed data show a good agreement with observations although the The shorter and coarser ERA-Interim reanalysis outperforms the hindcast in many aspects. The main advantages of this shows smaller errors for most locations and outperforms the coastDat2 hindcast in open waters. For coastal locations, for which unresolved bathymetry and land-sea distribution in ERA-Interim may play a role, improvements in coastDat2 are visible. Whereas the ERA-Interim wave product generally underestimates extreme significant wave heights, the coastDat2 hindcast has a tendency to overestimate. This is consistent with results from an analysis of marine wind fields used as forcing data which also showed some overestimation of the more severe wind speeds (Geyer et al., 2015). Compared to its predecessor the coastDat1 wave hindcast Weisse and Günther (2007), which terminates in 2007, the coastDat2 hindcast shows similar and comparable performance (not shown).

One benefit of the coastDat2 wind-wave hindcast ~~are~~ is the extended period for which reconstructed wave data are available~~, the increased resolution both in space and time~~. In particular, the use for extreme value statistics or assessment of long-term variability and change require data sets as long as possible. Unfortunately, wave measurements to validate the hindcast over such extended periods of time are unavailable. There are, however, some indications that the data may be used for such analyses: The wave climate strongly depends on the wind climate and the quality and homogeneity of the wave hindcast is thus strongly coupled to those of the driving atmospheric data which are discussed in Geyer (2014) and in Geyer et al. (2015). In these papers, hindcast wind is compared with observations and for most locations, a slight overestimation and root mean square errors between 1.6 ms^{-1} and ~~the more comprehensive set of wave parameters available (Appendix B). In addition, the hindcast provides a more conservative estimates for extreme value analyses which in some circumstances might be of advantage. As an example, one might think of safety related assessments in offshore engineering.~~ 3.4 ms^{-1} were found. Moreover, the described long-term (decadal) variability, closely resembles the known variations in storm activity over the North Sea. The latter was shown to occur also for waves in a hindcast that uses wind fields from a different regional atmosphere model that was, however, driven by the same global reanalysis (Weisse and Günther, 2007).

Regarding homogeneity Kistler et al. (2001) investigated the issue for the global NCEP reanalysis that provided the boundaries for the regional atmosphere models used in this and the study of Weisse and Günther (2007). Kistler et al. (2001) showed that the skill for the Northern Hemisphere rapidly increased from 1948 to 1958 while there is only a small increase afterwards. The latter implies that the driving global reanalysis is mostly homogeneous for our area after about 1958 and, as there were no changes in regional model systems used in Geyer (2014) and our study, we conclude that the same may also hold for our wave hindcast.

As part of a comprehensive approach to consistently reconstruct atmospheric (Geyer, 2014), tide-surge (Gaslikova and Weisse, 2013) and wind-waves conditions (this paper), the hindcast contributes to a consistent met-ocean ~~data set~~ dataset that provides a useful data source for analysing long-term meteo-marine climate variability and change. Furthermore, it represents a valuable source of data for a large variety of related and more applied research in the industry and administration (Weisse et al., 2015). As part of the coastDat2 dataset, data from the described wind-wave hindcast (Groll and Weisse, 2016) are freely available and can be accessed from doi:10.1594/WDCCcoastDat2_WAM–North_Sea.

Appendix A: Error metrics

To evaluating the skill of the wave model standard statistical measures are used. The mean $(\overline{E})$, the standard deviation (SD), the bias, the root mean square error $(RMSE)$, the scatter index (SI) and the correlation coefficient (r) are defined as follows

$$~~mean~~\overline{E} = \frac{\sum_{i=1}^{n} E_i}{n} \tag{A1}$$

$$SD = \sqrt{\frac{\sum_{i=1}^{n} (E_i - \overline{E})^2}{n}} \tag{A2}$$

$$bias = \frac{\sum_{i=1}^{n}(E_i - R_i)}{n} \tag{A3}$$

$$RMSE = \sqrt{\frac{\sum_{i=1}^{n}(E_i - R_i)^2}{n}} \tag{A4}$$

$$SI = \frac{RMSE}{\overline{R}} \tag{A5}$$

$$r = \frac{\sum_{i=1}^{n}(E_i - \overline{E})(R_i - \overline{R})}{\sqrt{\sum_{i=1}^{n}(E_i - \overline{E})^2 \sum_{i=1}^{n}(R_i - \overline{R})^2}} \tag{A6}$$

where the overlines indicate mean values over time, n denotes the number of data pairs, E refers to the estimator (coastDat2 or ERA-Interim) and R refers to the reference data (in situ or satellite observations). If coastDat2 is compared to ERA-Interim, the later is used as the reference data R. Using the decomposition of the mean squared error (MSE) into variance (VAR) and $bias$ ($MSE = VAR + bias^2$), the standard deviation of the error (SDE) is used as an estimate for the unbiased $RMSE$ and is defined as

$$SDE = \sqrt{RMSE^2 - ME^2}\sqrt{RMSE^2 - bias^2} \tag{A7}$$

Appendix B: Available variables

See Table B1.

Acknowledgements. We thank the providers of the observational data, namely, the Bundesamt für Seeschifffahrt und Hydrographie (BSH), the Norwegian Meteorological Institute, the Royal Netherlands Meteorological Institute (KNMI), the European Space Agency (ESA) and the French Research Institute for Exploitation of the Sea (IFREMER) for their support. We also thank the providers of the numerical data, namely, the European Centre for Medium-Range Weather Forecasts (ECMWF) for the ERA-Interim reanalysis data and the Met Office Hadley Centre for Climate Science and Services for access to the sea ice data setdataset.

References

Bertin, X., Prouteau, E., and Letetrel, C.: A significant increase in wave height in the North Atlantic Ocean over the 20th century, Global and Planetary Change, 106, 77 – 83, doi:http://dx.doi.org/10.1016/j.gloplacha.2013.03.009, http://www.sciencedirect.com/science/article/pii/S092181811300088X, 2013.

Bidlot, J., Janssen, P., and Abdalla, S.: A revised formulation for ocean wave dissipation in CY29R1, ECMWF Technical Memorandum, R60.9/JB/0516, 2005.

Bidlot, J., Janssen, P., and Abdalla, S.: A revised formulation for ocean wave dissipation and its model impact, ECMWF Technical Memorandum, 509, 2007.

Charles, E., Idier, D., Thiébot, J., Cozannet, G. L., Pedreros, R., Ardhuin, F., and Planton, S.: Present Wave Climate in the Bay of Biscay: Spatiotemporal Variability and Trends from 1958 to 2001, Journal of Climate, 25, 2020–2039, doi:10.1175/JCLI-D-11-00086.1, http://dx.doi.org/10.1175/JCLI-D-11-00086.1, 2012.

Chawla, A., Spindler, D. M., and Tolman, H. L.: Validation of a thirty year wave hindcast using the Climate Forecast System Reanalysis winds, Ocean Modelling, 70, 189 – 206, doi:http://dx.doi.org/10.1016/j.ocemod.2012.07.005, http://www.sciencedirect.com/science/article/pii/S1463500312001047, 2013.

Cox, A. T. and Swail, V. R.: A global wave hindcast over the period 1958–1997: Validation and climate assessment, Journal of Geophysical Research: Oceans, 106, 2313–2329, doi:10.1029/2001JC000301, http://dx.doi.org/10.1029/2001JC000301, 2001.

Dee, D. P., Uppala, S. M., Simmons, A. J., Berrisford, P., Poli, P., Kobayashi, S., Andrae, U., Balmaseda, M. A., Balsamo, G., Bauer, P., Bechtold, P., Beljaars, A. C. M., van de Berg, L., Bidlot, J., Bormann, N., Delsol, C., Dragani, R., Fuentes, M., Geer, A. J., Haimberger, L., Healy, S. B., Hersbach, H., Hólm, E. V., Isaksen, L., Kållberg, P., Köhler, M., Matricardi, M., McNally, A. P., Monge-Sanz, B. M., Morcrette, J.-J., Park, B.-K., Peubey, C., de Rosnay, P., Tavolato, C., Thépaut, J.-N., and Vitart, F.: The ERA-Interim reanalysis: configuration and performance of the data assimilation system, Quarterly Journal of the Royal Meteorological Society, 137, 553–597, doi:10.1002/qj.828, http://dx.doi.org/10.1002/qj.828, 2011.

Dodet, G., Bertin, X., and Taborda, R.: Wave climate variability in the North-East Atlantic Ocean over the last six decades, Ocean Modelling, 31, 120 – 131, doi:http://dx.doi.org/10.1016/j.ocemod.2009.10.010, http://www.sciencedirect.com/science/article/pii/S1463500309002066, 2010.

Feser, F., Weisse, R., and von Storch, H.: Multi-decadal atmospheric modeling for Europe yields multi-purpose data, EOS Transactions, 82, 305–310, 2001.

Gaslikova, L. and Weisse, R.: coastDat-2 TRIM-NP-2d Tide-Surge North Sea, World Data Center for Climate, doi:10.1594/WDCC/coastDat-2_TRIM-NP-2d., http://dx.doi.org/doi:10.1594/WDCC/coastDat-2_TRIM-NP-2d, 2013.

Geyer, B.: High-resolution atmospheric reconstruction for Europe 1948–2012: coastDat2, Earth System Science Data, 6, 147–164, doi:10.5194/essd-6-147-2014, http://www.earth-syst-sci-data.net/6/147/2014/, 2014.

Geyer, B., Weisse, R., Bisling, P., and Winterfeldt, J.: Climatology of North Sea wind energy derived from a model hindcast for 1958–2012, Journal of Wind Engineering and Industrial Aerodynamics, 147, 18 – 29, doi:http://dx.doi.org/10.1016/j.jweia.2015.09.005, http://www.sciencedirect.com/science/article/pii/S0167610515002214, 2015.

Groll, N. and Weisse, R.: coastDat-2 North Sea wave hindcast for the period 1949-2014 performed with the wave model WAM, World Data Center for Climate, doi:10.1594/WDCC/coastDat-2_WAM-North_Sea, http://dx.doi.org/10.1594/WDCC/coastDat-2_WAM-North_Sea, 2016.

Holthuijsen, L. H.: Waves in oceanic and coastal waters, Cambridge University Press, 2007.

Kalnay, E., Kanamitsu, M., Kistler, R., Collins, W., Deaven, D., Gandin, L., Iredell, M., Saha, S., White, G., Woollen, J., Zhu, Y., Leetmaa, A., Reynolds, R., Chelliah, M., Ebisuzaki, W., Higgins, W., Janowiak, J., Mo, K. C., Ropelewski, C., Wang, J., Jenne, R., and Joseph, D.: The NCEP/NCAR 40-Year Reanalysis Project, Bulletin of the American Meteorological Society, 77, 437–471, doi:10.1175/1520-0477(1996)077<0437:TNYRP>2.0.CO;2, http://dx.doi.org/10.1175/1520-0477(1996)077<0437:TNYRP>2.0.CO;2, 1996.

Kettle, A. J.: Review Article: Storm Britta in 2006: offshore damage and large waves in the North Sea, Natural Hazards and Earth System Sciences Discussions, 3, 5493–5510, doi:10.5194/nhessd-3-5493-2015, http://www.nat-hazards-earth-syst-sci-discuss.net/3/5493/2015/, 2015.

Kistler, R., Collins, W., Saha, S., White, G., Woollen, J., Kalnay, E., Chelliah, M., Ebisuzaki, W., Kanamitsu, M., Kousky, V., van den Dool, H., Jenne, R., and Fiorino, M.: The NCEP–NCAR 50–Year Reanalysis: Monthly Means CD–ROM and Documentation, Bulletin of the American Meteorological Society, 82, 247–267, doi:10.1175/1520-0477(2001)082<0247:TNNYRM>2.3.CO;2, http://dx.doi.org/10.1175/1520-0477(2001)082<0247:TNNYRM>2.3.CO;2, 2001.

Komen, G., Cavaleri, L., Hasselmann, H., Hasselmann, S., and Janssen, P.: Dynamics and Modelling of Ocean Waves, Cambridge University Press, 1996.

Neumann, D., Matthias, V., Bieser, J., Aulinger, A., and Quante, M.: A comparison of sea salt emission parameterizations in northwestern Europe using a chemistry transport model setup, Atmospheric Chemistry and Physics, 16, 9905–9933, doi:10.5194/acp-16-9905-2016, http://www.atmos-chem-phys.net/16/9905/2016/, 2016.

Ponce de León, S. and Guedes Soares, C.: Hindcast of extreme sea states in North Atlantic extratropical storms, Ocean Dynamics, 65, 241–254, doi:10.1007/s10236-014-0794-6, http://dx.doi.org/10.1007/s10236-014-0794-6, 2015.

Queffeulou, P.: Merged altimeter wave height data base. An update., in: ESA Living Planet Symposium 2013, Edinburgh, UK 9–13 September 2013, ESA SP-722, ftp://ftp.ifremer.fr/ifremer/cersat/products/swath/altimeters/waves/documentation/publications/ESA_Living_Planet_Symposium_2013.pdf, 2013.

Rayner, N. A., Parker, D. E., Horton, E. B., Folland, C. K., Alexander, L. V., Rowell, D. P., Kent, E. C., and Kaplan, A.: Global analyses of sea surface temperature, sea ice, and night marine air temperature since the late nineteenth century, Journal of Geophysical Research: Atmospheres, 108, n/a–n/a, doi:10.1029/2002JD002670, http://dx.doi.org/10.1029/2002JD002670, 4407, 2003.

Reguero, B., Menéndez, M., Méndez, F., Mínguez, R., and Losada, I.: A Global Ocean Wave (GOW) calibrated reanalysis from 1948 onwards, Coastal Engineering, 65, 38 – 55, doi:http://dx.doi.org/10.1016/j.coastaleng.2012.03.003, http://www.sciencedirect.com/science/article/pii/S0378383912000452, 2012.

Reguero, B., Méndez, F., and Losada, I.: Variability of multivariate wave climate in Latin America and the Caribbean, Global and Planetary Change, 100, 70 – 84, doi:http://dx.doi.org/10.1016/j.gloplacha.2012.09.005, http://www.sciencedirect.com/science/article/pii/S0921818112001828, 2013.

Reistad, M., Breivik, O., Haakenstad, H., Aarnes, O. J., Furevik, B. R., and Bidlot, J.-R.: A high-resolution hindcast of wind and waves for the North Sea, the Norwegian Sea, and the Barents Sea, Journal of Geophysical Research: Oceans, 116, n/a–n/a, doi:10.1029/2010JC006402, http://dx.doi.org/10.1029/2010JC006402, c05019, 2011.

Schwichtenberg, F., Callies, U., Groll, N., and Maßmann, S.: Effects of chemical dispersants on oil spill drift paths in the German Bight—probabilistic assessment based on numerical ensemble simulations, Geo-Marine Letters, pp. 1–8, doi:10.1007/s00367-016-0454-6, http://dx.doi.org/10.1007/s00367-016-0454-6, 2016.

Sterl, A., Komen, G. J., and Cotton, P. D.: Fifteen years of global wave hindcasts using winds from the European Centre for Medium-Range Weather Forecasts reanalysis: Validating the reanalyzed winds and assessing the wave climate, Journal of Geophysical Research: Oceans, 103, 5477–5492, doi:10.1029/97JC03431, http://dx.doi.org/10.1029/97JC03431, 1998.

Uppala, S. M., KÅllberg, P. W., Simmons, A. J., Andrae, U., Bechtold, V. D. C., Fiorino, M., Gibson, J. K., Haseler, J., Hernandez, A., Kelly, G. A., Li, X., Onogi, K., Saarinen, S., Sokka, N., Allan, R. P., Andersson, E., Arpe, K., Balmaseda, M. A., Beljaars, A. C. M., Berg, L. V. D., Bidlot, J., Bormann, N., Caires, S., Chevallier, F., Dethof, A., Dragosavac, M., Fisher, M., Fuentes, M., Hagemann, S., Hólm, E., Hoskins, B. J., Isaksen, L., Janssen, P. A. E. M., Jenne, R., Mcnally, A. P., Mahfouf, J.-F., Morcrette, J.-J., Rayner, N. A., Saunders, R. W., Simon, P., Sterl, A., Trenberth, K. E., Untch, A., Vasiljevic, D., Viterbo, P., and Woollen, J.: The ERA-40 re-analysis, Quarterly Journal of the Royal Meteorological Society, 131, 2961–3012, doi:10.1256/qj.04.176, http://dx.doi.org/10.1256/qj.04.176, 2005.

von Storch, H., Langenberg, H., and Feser, F.: A Spectral Nudging Technique for Dynamical Downscaling Purposes, Monthly Weather Review, 128, 3664–3673, doi:10.1175/1520-0493(2000)128<3664:ASNTFD>2.0.CO;2, http://dx.doi.org/10.1175/1520-0493(2000)128<3664:ASNTFD>2.0.CO;2, 2000.

WAMDI-Group: The WAM model – a third generation ocean wave prediction model, J Phys Oceanogr, 18, 1776–1810, 1988.

WASA-Group: Changing Waves and Storms in the Northeast Atlantic?, Bulletin of the American Meteorological Society, 79, 741–760, doi:10.1175/1520-0477(1998)079<0741:CWASIT>2.0.CO;2, http://dx.doi.org/10.1175/1520-0477(1998)079<0741:CWASIT>2.0.CO;2, 1998.

Weisse, R. and Günther, H.: Wave climate and long-term changes for Southern North Sea obtained from a high-resolution hindcast 1958-2002, Ocean Dynamics, 57, 161–172, doi:10.1007/s10236-006-0094-x, 2007.

Weisse, R. and Plüss, A.: Storm-related sea level variations along the North Sea coast as simulated by a high-resolution model 1958–2002, Ocean Dynamics, 56, 16–25, doi:10.1007/s10236-005-0037-y, http://dx.doi.org/10.1007/s10236-005-0037-y, 2006.

Weisse, R., von Storch, H., Callies, U., Chrastansky, A., Feser, F., Grabemann, I., Günther, H., A. Plüss, T. S., Tellkamp, J., Winterfeldt, J., and Woth, K.: Regional meteorological-marine reanalysis and climate change projections. Results for northern Europe and potential for coastal and offshore applications, Bulletin of the Amer. Met. Soc., 90, 849–860, doi:10.1175/2008BAMS2713.1, 2009.

Weisse, R., Bisling, P., Gaslikova, L., Geyer, B., Groll, N., Hortamani, M., Matthias, V., Maneke, M., Meinke, I., Meyer, E. M., Schwichtenberg, F., Stempinski, F., Wiese, F., and Wöckner-Kluwe, K.: Climate services for marine applications in Europe, Earth Perspectives, 2, 1–14, doi:10.1186/s40322-015-0029-0, http://dx.doi.org/10.1186/s40322-015-0029-0, 2015.

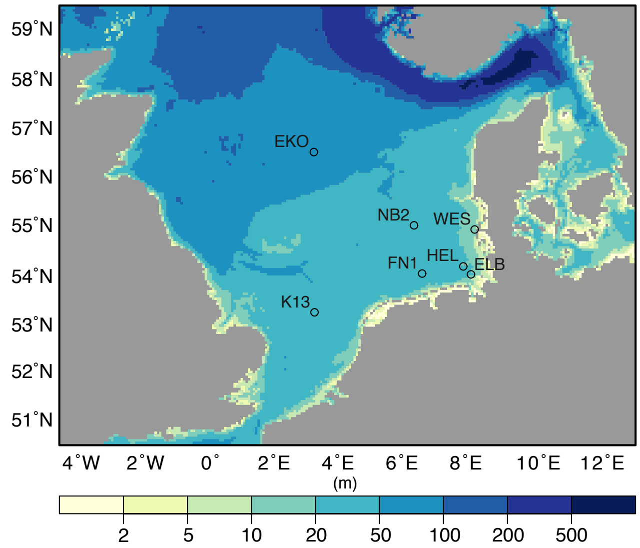

Figure 1. Model domain and bathymetry used for the fine grid simulation. Colours indicate water depth in meters. Circles mark observational sites used for the model evaluation. For the abbreviations see Tab. 1.

Table 1. Location and description of in situ measurements used for comparison.

site	location	depth [m]	time period	type
EKO	2.6°E / 56.5°N	72	1980-1998	platform
K13	3.2°E / 53.2°N	25	1980-2008	platform
NB2	6.3°E / 55.0°N	42	1993-2012	buoy
FN1	6.6°E / 54.0°N	30	2003-2012	platform
HEL	7.9°E / 54.2°N	20	1989-2012	buoy
ELB	8.1°E / 54.0°N	25	1990-2012	buoy
WES	8.2°E / 54.9°N	14	1993-2012	buoy

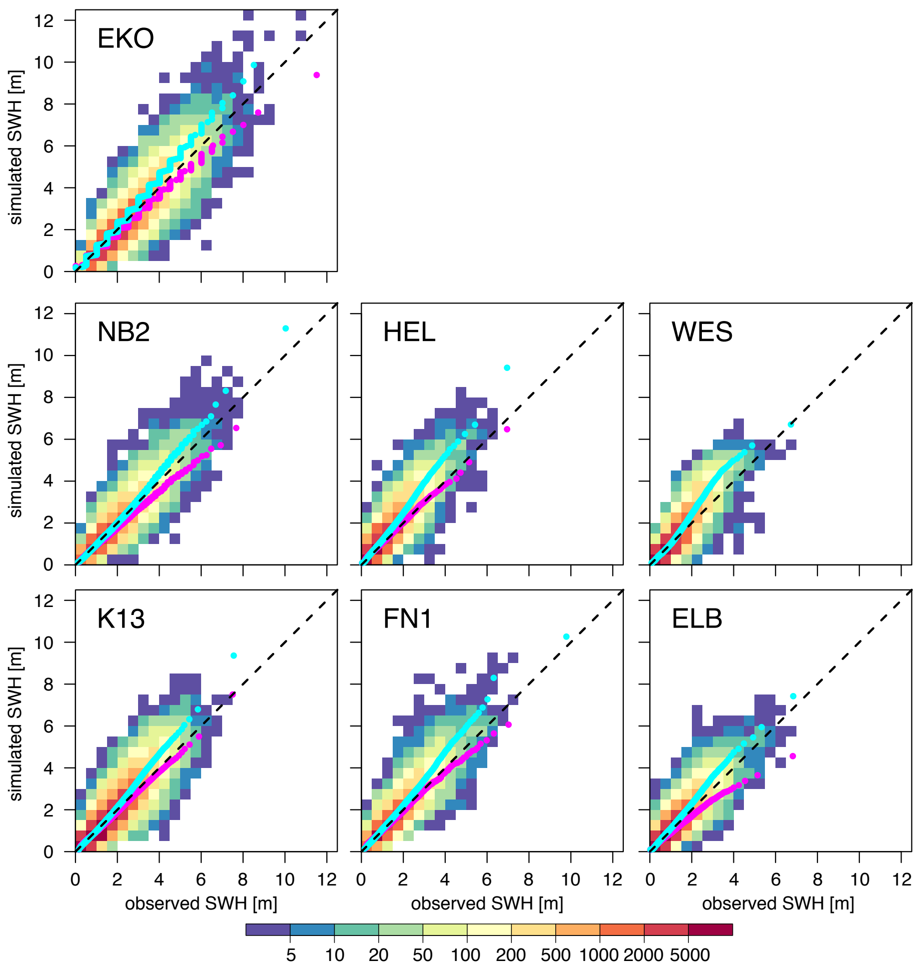

Figure 2. Scatter and quantile-quantile plot of ~~observed~~ SWH [m] between in situ observation (x-axis) and coastDat2 hindcast data (y-axis)~~SWH~~. Coloured squares indicate the number of data in each 0.5 m x 0.5 m bin. Coloured dots represent the percentile values of the quantile-quantile plots between observed and coastDat2 hindcast (cyan) and between observed and ERA-Interim reanalysis significant wave heights (magenta). Note that the comparison is made for different periods according to data availability (see Table 1).

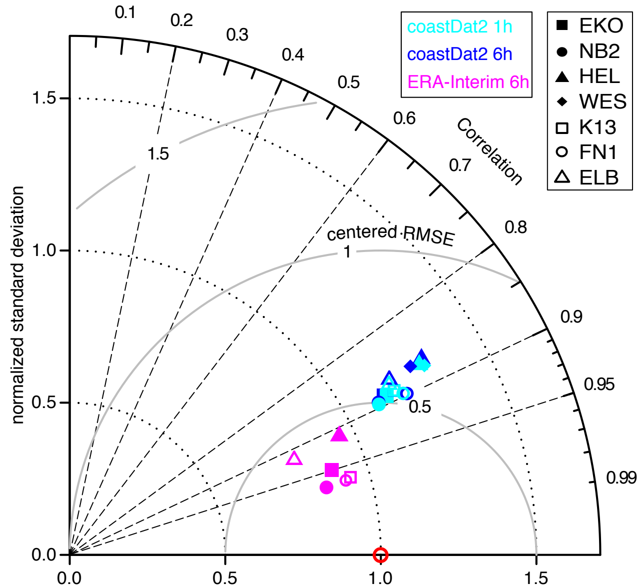

Figure 3. Normalized Taylor diagram from hourly (cyan) and six hourly (blue) coastDat2 SWHs and from six-hourly ERA-Interim (magenta) SWHs at seven (coastDat2) and at six (ERA-Interim) observational sites. The red circle would represent a perfect model compared to the observations.

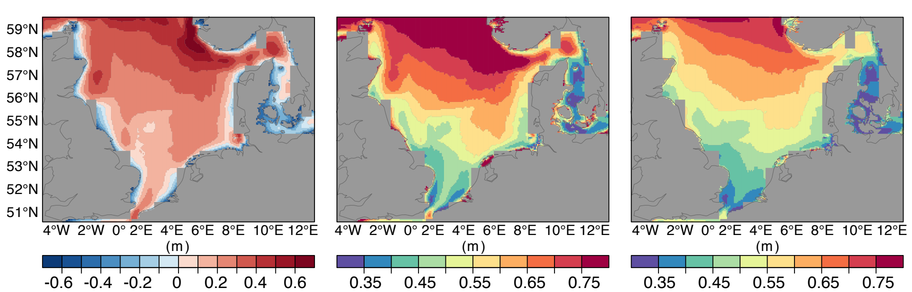

Figure 4. Spatial distribution of bias (left), root mean square distance (middle) and standard deviation of the error (right) [m] between SWHs derived from the coastDat2 hindcast and the ERA-Interim reanalysis for the period 1980–2014.

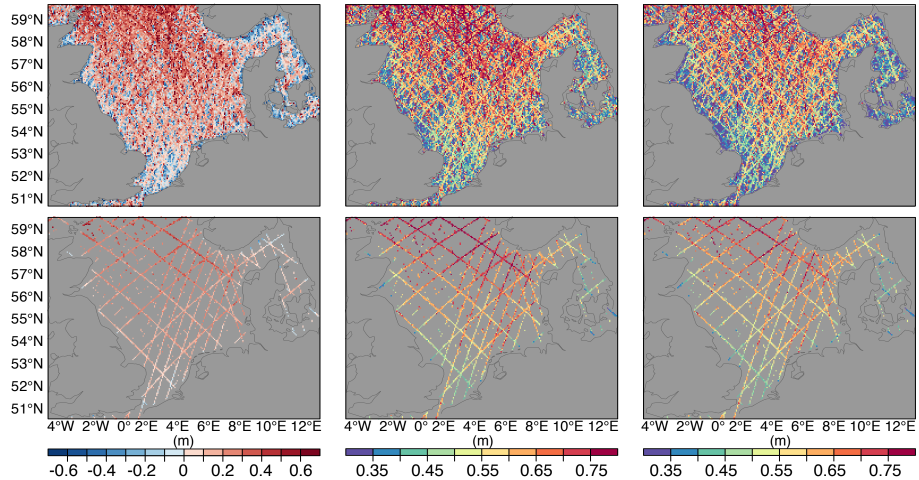

Figure 5. Spatial distribution of bias (left), root mean square error (middle) and standard deviation of the error (right) [m] between SWHs from the coastDat2 hindcast and the GlobWave ~~data set~~ dataset for the period 1992 – 2014 when all available satellite data are used for comparison (top) and when only data with more than 100 flyovers per grid point are used (bottom).

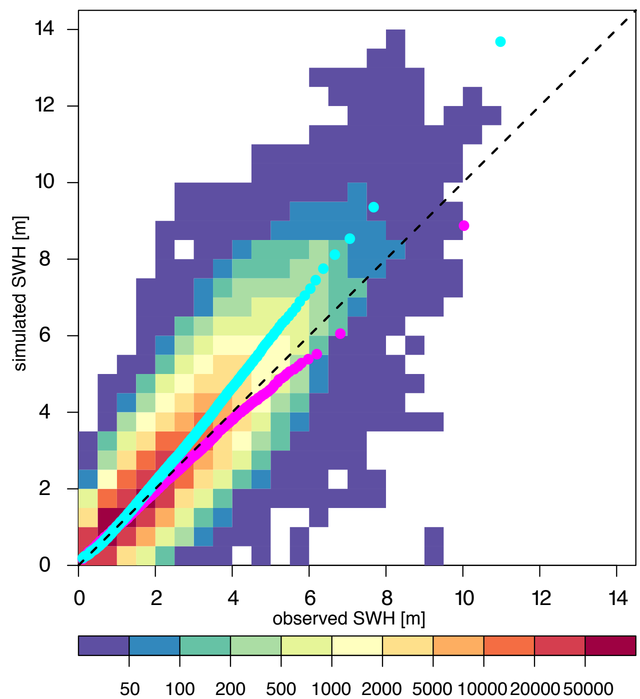

Figure 6. Scatter and quantile-quantile plot of ~~observed~~ SWH [m] between altimeter (GLOBWAVE) observation (x-axis) and coastDat2 hindcast data (y-axis)~~SWH~~. Coloured squares indicate the number of the data in each 0.5 m x 0.5 m bin. Coloured dots represent the percentile values of the quantile-quantile plots between observed and coastDat2 hindcast significant wave heights (cyan) and between observed and ERA-Interim SWH (magenta).

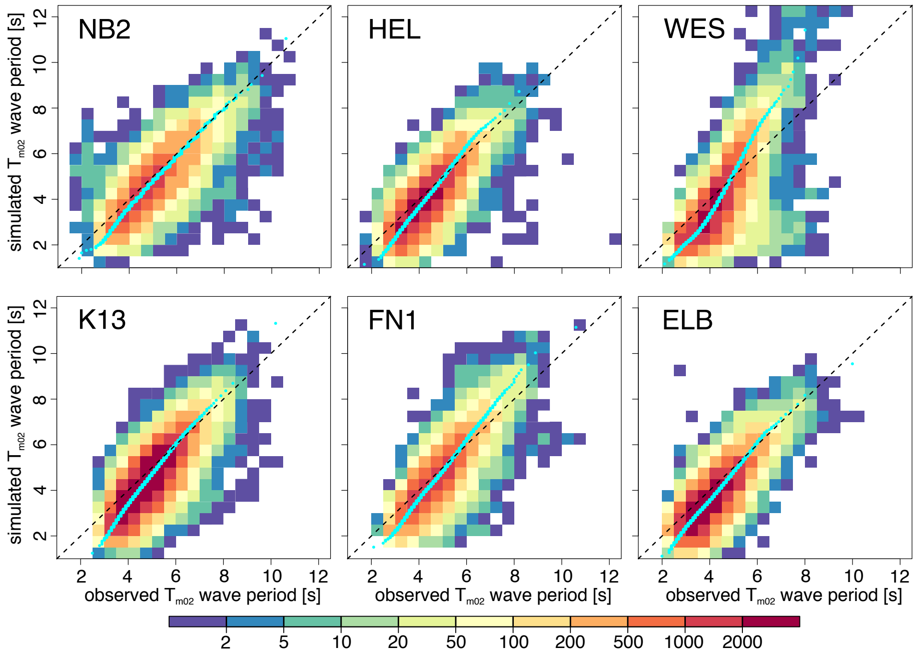

Figure 7. Scatter and quantile-quantile plot of ~~observed~~ T_{m02} wave period [s] between in situ observation (x-axis) and coastDat2 hindcast data (y-axis)~~T_{m02} wave period~~. Coloured squares indicate the density of the data in each 0.5 s x 0.5 s bin. Coloured dots represent the percentile values of the quantile-quantile plots between observed and coastDat2 hindcast T_{m02} (cyan) wave periods. Note that the comparison is made for different periods according to data availability (see Table 1).

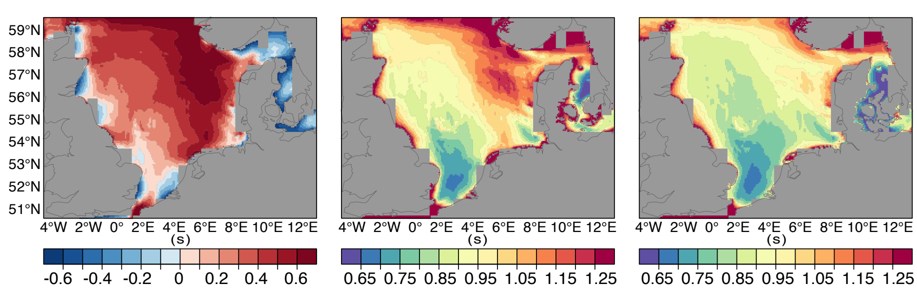

Figure 8. Spatial distribution of bias (left), root mean square error (middle) and standard deviation of the error (right) [s], between the mean wave period between from the coastDat2 hindcast and ERA-Interim reanalysis for the period 1980 – 2014.

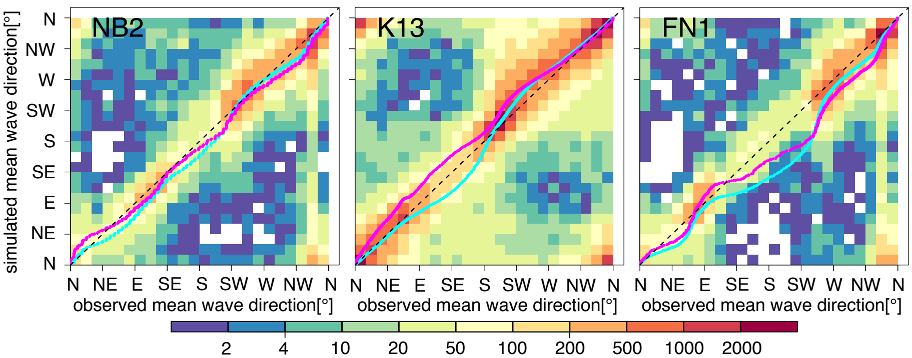

Figure 9. Scatter and quantile-quantile plot of ~~observed~~ mean wave direction between in situ observation (x-axis) and coastDat2 hindcast data (y-axis)~~mean wave direction~~. Coloured squares indicate the number of counts in each 15°x 15°bin. Coloured dots represent the percentile values of the quantile-quantile plots between observed and coastDat2 hindcast mean wave directions (cyan) and between observed and ERA-Interim mean wave directions (magenta). Note that the comparison is made for different periods according to data availability (see Table 1).

Table 2. Error metrics for the SWH at seven locations derived from in situ observations (OBS), coastDat2 hindcast (CD2) and ERA-Interim reanalysis (ERAi), for hourly (coastDat2) and six-hourly (ERA-Interim) data respectively.

name	count CD2/ERAi	mean [m] OBS/ CD2/ ERAi	standard deviation [m] OBS/ CD2/ ERAi	bias [m] CD2/ ERAi	RMSE [m] CD2/ ERAi	scatter index CD2/ ERAi	correlation CD2/ ERAi
EKO	51620/ 22589	2.08/ 2.24/ 1.94	1.29/ 1.48/ 1.15	0.16/ -0.14	0.71/ 0.44	0.34/ 0.21	0.88/ 0.95
K13	84744/ 42372	1.5/ 1.59/ 1.43	0.92/ 1.08/ 0.86	0.09/ -0.07	0.51/ 0.26	0.34/ 0.17	0.88/ 0.96
NB2	28485/ 5245	1.75/ 1.77/ 1.51	1.11/ 1.23/ 0.91	0.03/ -0.17	0.56/ 0.35	0.32/ 0.21	0.89/ 0.97
FN1	30893/ 4655	1.52/ 1.68/ 1.5	0.97/ 1.16/ 0.9	0.16/ -0.03	0.56/ 0.26	0.37/ 0.17	0.89/ 0.96
HEL	46074/ 14208	1.09/ 1.34/ 1.15	0.76/ 0.98/ 0.71	0.25/0.06	0.55/ 0.32	0.5/ 0.29	0.87/ 0.91
ELB	55190/ 14292	1.04/ 1.18/ 0.92	0.73/ 0.85/ 0.56	0.13/ -0.12	0.44/ 0.32	0.42/ 0.31	0.87/ 0.92
WES	43979/ NA	1.08/ 1.2/ NA	0.72/ 0.94/ NA	0.12/ NA	0.48/ NA	0.45/ NA	0.88/ NA
SAT	901451/ 82067	1.76/ 1.94/ 1.69	1.11/ 1.34/ 0.97	0.18/ -0.06	0.64/ 0.36	0.37/ 0.20	0.89/ 0.94

NA-not available

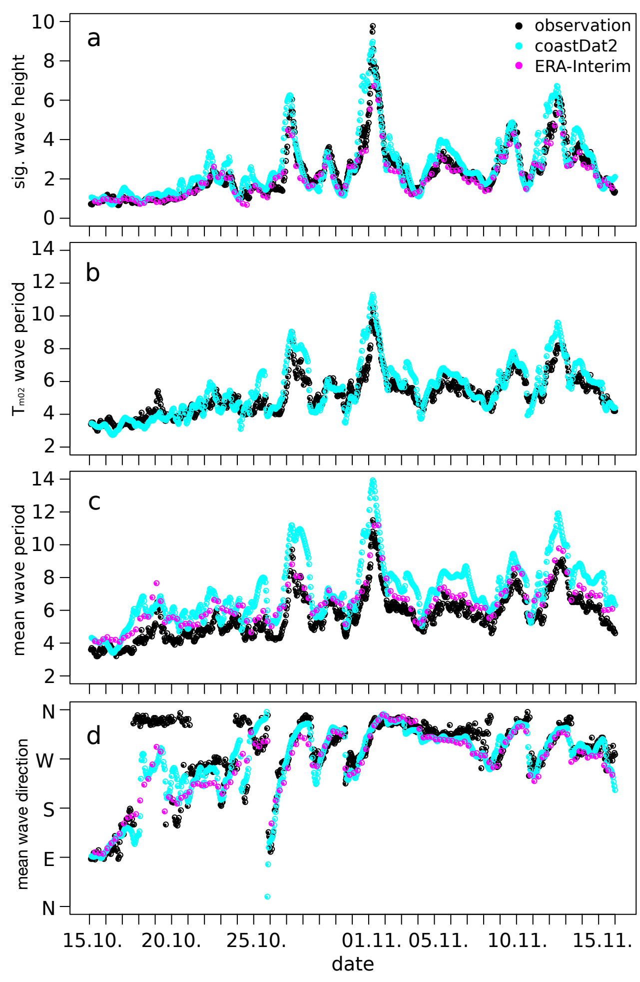

Figure 10. Time series of significant wave height [m] (a), T_{m02} [s] (b) and mean wave period [s] (c) and mean wave direction [°] (d) at FN1 for the period 15 October 2006, 00:00 UTC to 15 November 2006, 00:00 UTC. Observations are shown in black (a–d), the coastDat2 hindcast is shown in cyan (a–d) and the ERA-Interim data are shown in magenta (a,c,d).

Table 3. Error metrics for the T_{m02} period at six locations derived from in situ observations (OBS) and coastDat2 hindcast (CD2) data for hourly values.

name	count CD2	mean [s] OBS/ CD2	standard deviation [s] OBS/ CD2	bias [s] CD2	RMSE [s] CD2	scatter index CD2	correlation CD2
K13	84744	4.76 / 4.37	0.91/ 1.21	-0.39	0.84	0.18	0.79
NB2	28485	4.92/ 4.65	1.19/ 1.34	-0.27	0.87	0.18	0.79
FN1	30893	4.72/ 4.51	1.05/1.14	-0.21	0.82	0.17	0.82
HEL	46074	4.32/ 3.93	0.93/ 1.21	-0.30	0.81	0.19	0.78
ELB	55190	4.03/ 3.6	0.92/ 1.12	-0.43	0.82	0.20	0.78
WES	43979	4.22/ 3.83	0.89/ 1.48	-0.40	1.07	0.25	0.76

Table 4. Error metrics for the MWP at four locations derived from in situ observations (OBS), coastDat2 hindcast (CD2) and ERA-Interim (ERAi) data for hourly (coastDat2) and six-hourly (ERA-Interim) data, respectively.

name	count CD2/ERAi	mean [s] OBS/ CD2/ ERAi	standard deviation [s] OBS/ CD2/ ERAi	bias [s] CD2/ ERAi	RMSE [s] CD2/ ERAi	scatter index CD2/ ERAi	correlation CD2/ ERAi
NB2	28485/ 5254	5.25/ 6.16/ 5.75	1.23/ 1.54/ 1.2	0.91/ 0.59	1.31/ 0.83	0.25/ 0.16	0.79/ 0.88
FN1	30893/ 4655	5.11/ 6.14/ 5.75	1.19/ 1.66/ 1.21	1.04/ 0.62	1.41/ 0.8	0.28/0.16	0.82/ 0.91
ELB	55190/ 14292	4.32/ 4.99/ 4.96	1.02/ 1.39/ 1.05	0.67/ 0.63	1.08/ 0.87	0.25/ 0.2	0.8/ 0.83
WES	43979/ NA	4.58/ 5.45/ NA	1.02/ 1.77/ NA	0.87/ NA	1.46/ NA	0.32/ NA	0.78/ NA

NA-not available

Table 5. Error metrics for the mean wave direction at three locations derived from in situ observations (OBS), coastDat2 hindcast (CD2) and ERA-Interim (ERAi) data for hourly (coastDat2) and six-hourly (ERA-Interim) data, respectively.

name	count CD2/ERAi	mean [°] OBS/ CD2/ ERAi	standard deviation [°] OBS/ CD2/ ERAi	bias [°] CD2/ ERAi	RMSE [°] CD2/ ERAi	scatter index CD2/ ERAi	correlation CD2/ ERAi
NB2	28485/ 5254	241/ 233/ 226	99/ 100/ 95	26/ 24	41/ 37	0.17/ 0.15	0.79/ 0.85
K13	84744/ 42372	204/ 205/ 217	113/ 117/ 107	25/ 22	40/ 35	0.20/ 0.17	0.82/ 0.86
FN1	30893/ 4655	254/ 238/ 235	102/ 105/ 97	24/ 26	38/ 38	0.15/ 0.15	0.83/ 0.85

Table B1. List of available variables

	Variable name	Unit	Long name	Standard name
1	dd	degree	wind direction	wind_to_direction
2	ds	degree	total directional spread	sea_surface_wave_directional_spread
3	ds_sea	degree	sea directional spread	sea_surface_wind_wave_directional_spread
4	ds_swell	degree	swell directional spread	sea_surface_swell_wave_directional_spread
5	ff	ms^{-1}	wind speed	wind_speed
6	fv	ms^{-1}	friction velocity	
7	hs	m	total significant wave height	sea_surface_wave_height
8	hs_sea	m	sea significant wave height	sea_surface_wind_wave_height
9	hs_swell	m	swell significant wave height	sea_surface_swell_wave_height
10	nws	none	normalised_wave_stress	normalised_wave_stress
11	thq	degree	total mean wave direction	sea_surface_wave_to_direction
12	thq_sea	degree	sea mean wave direction	sea_surface_wind_wave_to_direction
13	thq_swell	degree	swell mean wave direction	sea_surface_swell_wave_to_direction
14	tmp	s	total mean period	sea_surface_wave_mean_period_from_variance _spectral_density_inverse_frequency_moment
15	tmp_sea	s	sea mean period	sea_surface_wind_wave_mean_period_from_variance _spectral_density_inverse_frequency_moment
16	tmp_swell	s	swell mean period	sea_surface_swell_wave_mean_period_from_variance _spectral_density_inverse_frequency_moment
17	tm1	s	total m1-period	sea_surface_wave_mean_period_from_variance _spectral_density_first_frequency_moment
18	tm1_sea	s	sea m1-period	sea_surface_wind_wave_mean_period_from_variance _spectral_density_first_frequency_moment
19	tm1_swell	s	swell m1-period	sea_surface_swell_wave_mean_period_from_variance _spectral_density_first_frequency_moment
20	tm2	s	total m2-period	sea_surface_wave_mean_period_from_variance _spectral_density_second_frequency_moment
21	tm2_sea	s	sea m2-period	sea_surface_wind_wave_mean_period_from_variance _spectral_density_second_frequency_moment
22	tm2_swell	s	swell m2-period	sea_surface_swell_wave_mean_period_from_variance _spectral_density_second_frequency_moment
23	tp	s	total peak-period	sea_surface_wave_peak_period_from_variance_spectral_density
24	tp_sea	s	sea peak period	sea_surface_wind_wave_peak_period_from_variance_spectral_density
25	tp_swell	s	swell peak period	sea_surface_swell_wave_peak_period_from_variance_spectral_density